

Tumorigenesis and Neoplastic Progression

# Involvement of Matrix Metalloproteinase Activity in Hormone-Induced Mammary Tumor Regression

Marina Simian, Alfredo Molinolo, and  
Claudia Lanari

From the Laboratorio de Carcinogénesis Hormonal, Instituto de Biología y Medicina Experimental, Consejo Nacional de Investigaciones Científicas y Técnicas, Buenos Aires, Argentina

**Proteolytic activity and remodeling of the extracellular matrix are important players in tumor progression. However, to date the role of the extracellular matrix in tumor regression remains unresolved. To address this, we used a progesterone-dependent *in vivo* mouse mammary tumor line, C4-HD, which regresses in response to hormone therapy. Within the first 72 hours of treatment, massive apoptosis was accompanied by changes in the staining patterns of laminin and collagens I, III, and IV. We thus hypothesized that an increase in matrix metalloproteinase (MMP) activity could be involved in this process. This indeed was the case as the activities of MMP-2, -9, and -3 increased in regressing tumors, coinciding with the peak of apoptosis. Moreover, cell-cell interactions were disrupted during early hours of regression with E-cadherin levels reduced and fragmentation products detected during regression. Analysis of β-catenin revealed that although total levels within the tissue did not change, this molecule switched from being involved in cell-cell adhesion in the growing tumor to being expressed in the reactive stroma during regression. Our data provide a novel role for proteolytic activity in tumor regression and question the underlying principle for using MMP inhibitors in cancer treatment.** (Am J Pathol 2006; 168:270–279; DOI: 10.2353/ajpath.2006.050012)

Breast cancer is by far the most frequent cancer in women (22% of all cancers) in industrialized countries<sup>1</sup> and is the second leading cause of cancer death.<sup>2</sup> With the aim of developing rational treatments, great effort has been focused on studying the mechanisms involved in carcinogenesis and tumor progression. A thorough understanding of the events that lead to tumor regression and its regulation is particularly important given that,

once the tumor has disseminated to various body sites, surgery is no longer an option and that current treatments are based on the assumption of inducing tumor shrinkage.

The extracellular matrix (ECM) provides information that is essential for embryonic development, morphogenesis, and differentiation of organs and wound healing.<sup>3</sup> Matrix metalloproteinases (MMPs) are capable of digesting various components of the ECM and other molecules such as growth factors, cell surface receptors, and cell adhesion molecules and thus play a critical role in the regulation of these physiological processes.<sup>4</sup> MMPs have been implicated in tumor progression as playing a key role in invasion and metastasis.<sup>5</sup> Analysis of the levels of MMPs in both human and experimental tumors has revealed that they are expressed at elevated levels, and *in situ* hybridization studies have shown that they are mainly produced by the host stroma and not by cancer cells.<sup>6</sup> The generation and analysis of transgenic and knockout mice for both MMPs and TIMPs (tissue inhibitors of MMPs) have revealed that MMPs also play a key role in the process of carcinogenesis.<sup>7</sup> All this information has led to the development of synthetic MMP inhibitors that have been tested in several phase I and III clinical trials. The rationale is that if MMPs are involved in tumor growth and invasion, then inhibition of MMP activity should interfere with these processes and thus lead to tumor shrink-

---

Supported by grants from Secretaría de Ciencia y Tecnología (BID1201/OC-AR, PICT 02 05 12276) and by the Sales Foundation.

Accepted for publication July 21, 2005.

M.S. is a postdoctoral fellow of Consejo Nacional de Investigaciones Científicas y Técnicas; A.M. is associate researcher at IBYME-Consejo Nacional de Investigaciones Científicas y Técnicas, Fundación Sales; and C.L. is a member of the Research Career, Consejo Nacional de Investigaciones Científicas y Técnicas.

Current address of M.S.: Research Area, Instituto de Oncología Angel Roffo, Buenos Aires, Argentina.

Current address of A.M.: Oral and Pharyngeal Cancer Branch, National Institute of Dental and Craniofacial Research, National Institutes of Health, Bethesda, MD 20892-4340.

Address reprint requests to Marina Simian, Research Area, Instituto de Oncología Angel Roffo, Buenos Aires, Argentina. E-mail: marina.simian@galuzzi.com.

age. To date, however, the results have not been promising.<sup>8</sup>

We have developed a tumor model in which long-term administration of medroxyprogesterone acetate (MPA) to BALB/c mice induces ductal metastatic progestin-dependent mammary gland carcinomas that express high levels of estrogen and progesterone receptors (ER, PR).<sup>9,10</sup> Because estrogens and anti-progestins induce complete tumor regression,<sup>11,12</sup> our model system is very useful for studying not only the biology of hormone-dependent tumor growth but also its remission. The fact that this phenomenon implies a loss of tissue mass in response to a change in signaling led us to hypothesize that mechanisms similar to those implicated in postlactation mammary gland involution could play a role in mammary tumor regression. Involution is a process that involves a high level of tissue remodeling, including an increase in proteolytic activity and induction of massive apoptosis.<sup>13,14</sup> These experiments showed that the increase in proteolytic activity in the early hours of involution is responsible for the induction of apoptosis. Furthermore, the loss of contact with the basement membrane has been shown to induce apoptosis,<sup>15</sup> a process referred to as anoikis.

Although a role for proteolytic activity seems intuitive in any event that leads to tissue remodeling, the association between tumor shrinkage and proteolysis has not been investigated, perhaps because of the current paradigm linking proteolysis to tumor progression. The aim of the present study was to analyze the events that occur at the tissue level in relation to apoptosis, ECM composition, and cell-cell interactions within the first 72 hours of treatment. Our results show a role for proteolytic activity in tumor regression and question the use of MMP inhibitors as a treatment for cancer.

## Materials and Methods

### Animals

Two-month-old virgin female BALB/c mice (Instituto de Biología y Medicina Experimental Animal Facility) were used. The animals were housed in groups of four per cage in an air-conditioned room at  $20^{\circ}\text{C} \pm 2^{\circ}\text{C}$  under a 12-hour light/dark cycle with access to food and tap water *ad libitum*. Animal care and manipulation were in agreement with institutional guidelines and the Guide for the Care and Use of Laboratory Animals.<sup>16</sup>

### Tumors

The progestin-dependent C4-HD tumor line was selected for this study. This tumor line is a mammary ductal carcinoma induced by MPA in BALB/c mice, expresses ER and PR,<sup>17</sup> and is maintained by syngeneic transplants in MPA-treated mice.

## Hormones and Anti-Hormones Used in Treatments

MPA (Medrosterona; Gador Laboratories, Buenos Aires, Argentina) was administered subcutaneously as previously described.<sup>18</sup> 17-β-Estradiol (E<sub>2</sub>) (Sigma Co., St. Louis, MO) in 5-mg silastic pellets were implanted subcutaneously as previously described.<sup>11,19</sup> RU486, or mifepristone, (Sigma Co.) is a type II anti-progestin that forms complexes with PR that bind DNA but are unable to induce transcription. It also has anti-glucocorticoid effects.<sup>20</sup> RU486 was administered subcutaneously in daily doses of 6.5 mg/kg body weight in saline as previously described.<sup>19</sup>

## Experimental Design

Tumors were transplanted subcutaneously by trocar (1 to 2 mm<sup>2</sup>) in the right inguinal flank of 10-week-old virgin female BALB/c mice treated with 20 mg of MPA depot. Tumor size was measured every other day with a Vernier caliper (length and width). The treatments were started when the tumors reached a size of 100 to 150 mm<sup>2</sup>. MPA was removed from selected groups of two to three mice that were subsequently treated with RU486 or E<sub>2</sub> or blank silastic pellets for 6 to 7, 12, 24, 48, and 72 hours. Control animals were treated with saline or implanted with blank silastic pellets; no signs of regression were ever detected in control MPA-treated animals. Experiments were performed at least three independent times for each time point. Tumors were collected and cut into pieces to be either quick frozen for immunofluorescence and protein extraction or fixed in 10% buffered formalin and embedded in paraffin for histological studies.

## Morphological Studies and Apoptosis

The morphological features of both tumor parenchyma and stroma were evaluated in hematoxylin and eosin (H&E)-stained slides. Apoptosis was assessed as previously described.<sup>19</sup> Briefly, apoptosis was counted in 5-μm H&E-stained sections by direct evaluation of 10 high-power fields in at least three independent tumors for each time point. Apoptosis was identified by cell shrinkage and condensation, peripheral clumping or fragmentation of nuclear chromatin, and the presence of apoptotic bodies.<sup>21</sup> Apoptosis was expressed as (total number of cells in apoptosis × high-power field)/(total number of cells × high-power field). The TUNEL (terminal dUTP nick-end labeling) technique (Apoptag Plus; Oncor, Gaithersburg, MD) was performed to corroborate the morphological studies.

## Zymography

Tumor samples were homogenized on ice in RIPA buffer (50 mmol/L Tris, pH 8.0, containing 150 mmol/L NaCl, 0.1% sodium dodecyl sulfate, 0.5% deoxycholate, and 1% Nonidet P-40). The homogenates were centrifuged for 15 minutes at 4°C, and the supernatants were sub-

jected to electrophoresis on gelatin substrate gels [8.8% sodium dodecyl sulfate-polyacrylamide slab gels containing 1 mg/ml of gelatin or 1.6 mg/ml of  $\alpha$ -casein (both from Sigma)], as described previously.<sup>22,23</sup> Seventy  $\mu$ g of protein were loaded in each well. Subsequently, the gels were treated with 2.5% Triton X-100 for 30 minutes, followed by incubation for 24 hours at 37°C in a buffer containing 100 mmol/L Tris-HCl, pH 7.4, and 15 mmol/L CaCl<sub>2</sub>. The gels were stained with Coomassie Blue R-250 and destained with water until clear zones indicative of proteolytic activity emerged against a blue background. Bands were quantified using a densitometer (Molecular Analyst GS 700; Bio-Rad, Hercules, CA).

### Western Blot

Extracts were prepared by homogenizing tumor samples in phosphate-buffered saline (PBS) (pH 7.4), 1% Nonidet P-40, 0.5% deoxycholate, and 0.1% sodium dodecyl sulfate containing protease inhibitors (40  $\mu$ mol/L phenylmethyl sulfonyl fluoride, 5  $\mu$ g/ml leupeptin, 50  $\mu$ g/ml aprotinin, and 200  $\mu$ mol/L orthovanadate). Protein concentration was measured using the Lowry method. Samples were mixed with 4 $\times$  sample buffer containing  $\beta$ -mercaptoethanol and boiled for 2 minutes. Seventy  $\mu$ g of each sample were then separated in 6%, 8%, and 12% sodium dodecyl sulfate-polyacrylamide gel electrophoresis mini gels (Bio-Rad) and transferred to nitrocellulose membranes (Hybond-ECL; Amersham Biosciences, Uppsala, Sweden). The membranes were blocked overnight in 5% fat-free milk and 0.1% Tween-20 in PBS at 4°C. Primary antibodies were used at a 1:500 dilution in PBS containing 0.1% Tween-20 (PBST) and 2.5% fat-free milk and were incubated for 2 hours at room temperature. After washing with PBST, membranes were incubated with secondary antibodies at a 1:1000 dilution for 1 hour at room temperature. Signals were detected with an enhanced chemiluminescence kit (Super Signal; Pierce Biotechnology, Rockford, IL).

### Immunofluorescence

Frozen tumor samples were cut using a cryostat to obtain 10- to 12- $\mu$ m thick sections. They were air-dried and fixed for 20 minutes in 10% formalin in PBS. Subsequently, nonspecific binding sites were blocked by incubation in blocking buffer (PBS containing 2% fetal calf serum) for 1 hour at room temperature. Sections were then treated with primary antibodies dissolved in blocking buffer at a 1:100 dilution overnight at 4°C. After three washes in PBS, sections were incubated with fluorescein-conjugated secondary antibodies (1:100 dilution) for 1 hour at room temperature in blocking buffer. Slides were then washed with PBS, nuclei were stained with either propidium iodide or 4',6-diamino-2-phenylindole (Sigma), and slides were mounted with Vectashield (Vector Laboratories, Burlingame, CA). Sections were analyzed under a Nikon laser confocal microscope.

### Antibodies

The following primary antibodies were used for immunofluorescence studies: rabbit anti-laminin (E.Y. Laboratories, San Mateo, CA; a kind gift of Dr. Mina J. Bissell), rabbit anti-collagen IV (a kind gift of Dr. Mina J. Bissell), goat anti-collagen I (Pierce Biotechnology; a kind gift of Dr. Mary Helen Barcellos-Hoff), rabbit anti-E-cadherin (Santa Cruz Biotechnology, Santa Cruz, CA), and mouse anti- $\beta$ -catenin (BD Biosciences, San Diego, CA). The following secondary antibodies were used: fluorescein isothiocyanate (FITC)-conjugated goat anti-rabbit (Zymed, San Francisco, CA), FITC-conjugated rabbit anti-goat (Pierce Biotechnology, a kind gift of Dr. Mary Helen Barcellos-Hoff), and FITC-conjugated rabbit anti-mouse (Zymed). In experiments using the mouse anti- $\beta$ -catenin antibody, tissues were incubated with mouse-on-mouse reagent (M.O.M., Vector Laboratories) to block any endogenous mouse antibodies, as indicated by the manufacturer. For Western blots the following primary antibodies were used: rabbit anti-E-cadherin (Santa Cruz Biotechnology), mouse anti-E-cadherin (BD Biosciences), and mouse anti- $\beta$ -catenin (Becton-Dickinson Laboratories, Mountain View, CA). Secondary antibodies were peroxidase-conjugated goat anti-rabbit (Amersham) and rabbit anti-mouse (Amersham).

### Statistical Analysis

Data were analyzed using Graph Pad software. Two-way analysis of variance followed by Bonferroni's post test was applied, with  $P \leq 0.05$  considered significant.

### Results

#### Apoptosis and Tissue Remodeling during Mammary Tumor Regression

To study the events involved in hormone-dependent mammary tumor regression, we used the hormone-dependent C4-HD tumor model that is composed of roughly rounded cohesive groups of atypical glandular cells that occasionally show signs of tubular differentiation separated by scanty fibroblastic stroma (Figure 1A). Removal of MPA in mice carrying the C4-HD tumor led to partial tumor regression; however, additional treatment with E<sub>2</sub> or RU486 led to complete regression within 15 days (Figure 2). Figure 1, B, C, and D shows the histology of the regressing tumors, reflecting radical changes in morphology in the first 72 hours of treatment. To gain further insight into the mechanism of regression, we quantified the percentage of apoptotic cells within the first 72 hours of regression. Figure 3 shows that as early as 6 hours after the beginning of E<sub>2</sub> or RU486 treatments, or 12 hours for mice treated by only removing MPA, there was a statistically significant increase in the percentage of apoptotic cells compared to control groups. The maximum percentage of apoptotic cells for all treatments occurred at 48 hours, a time after which levels declined to

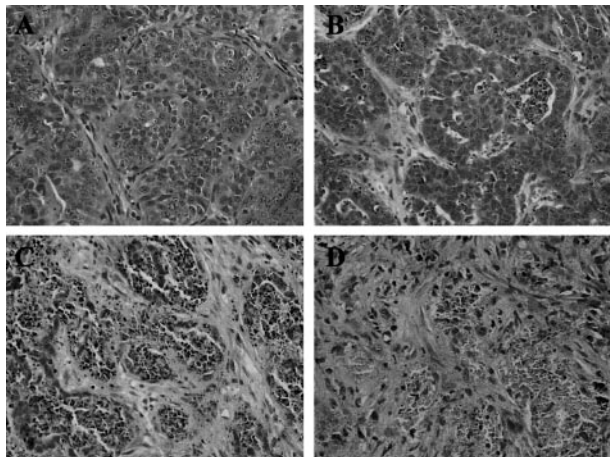


**Figure 1.** Histological appearance of the C4-HD tumor during growth and regression. BALB/c mice bearing the C4-HD tumor were treated by removing MPA or by adding estradiol ( $E_2$ ) or the anti-progestin RU486 for 12, 24, 48, or 72 hours to induce tumor regression. Tumors were collected, fixed in 10% formalin, embedded in paraffin, and processed according to standard procedures to obtain H&E-stained sections. **A:** Appearance of the growing C4-HD tumor (control) is characterized by groups of atypical cells with cribriform differentiation and occasional central necrosis. Stroma is fibroblastic and well vascularized. Atypical features, as well as several mitotic figures, are evident at high magnification. Representative H&E sections prepared from tumors derived from mice treated with RU486 for 12 (**B**), 24 (**C**), and 72 (**D**) hours are shown. Similar images were observed in the -MPA- and  $E_2$ -treated samples. **B:** At 12 hours the tumor shows round groups of cells with extensive apoptosis or central necrosis. The stroma is more abundant than the intercellular substance seems to have increased. **C:** By 24 hours only a few tumor cells appear viable. Many of them have undergone apoptosis or are part of a necrotic process. Stroma is very abundant and seems well vascularized. **D:** At 72 hours few viable tumor cells are evident. Cellular debris and apoptotic fragments are embedded in an abundant fibroblastic stroma. Original magnifications,  $\times 400$ .

those measured at 12 hours of treatment. The results obtained are consistent with the fact that by 72 hours histological analysis showed that most epithelial-like cells were lost (Figure 1D). This was further confirmed by keratin staining that showed a high number of keratin-

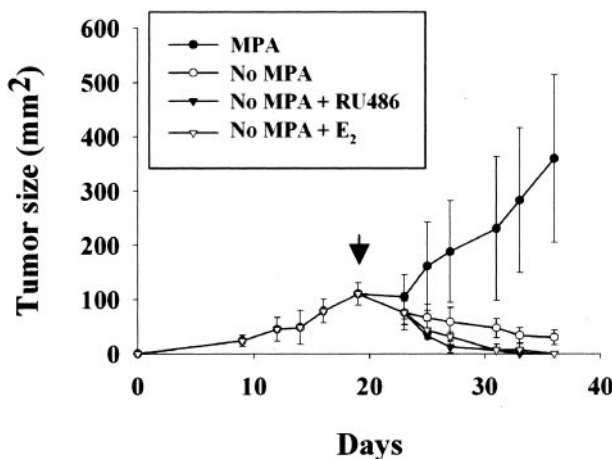


**Figure 2.** Growth and regression kinetics of the C4-HD tumor. The progestin-dependent C4-HD tumor was grown subcutaneously in 2-month-old virgin female nonovariectomized BALB/c mice until tumor size reached  $\sim 100 \text{ mm}^2$ . At this point, MPA depot was removed, and mice were further treated with  $E_2$  or RU486 or remained untreated. Control animals were sham operated and treated with vehicle alone. As shown in the figure, complete regression is achieved in both the  $E_2$ - and RU486-treated groups after 15 days. Each curve represents the mean  $\pm$  SD of three mice for each time point and treatment. The **arrow** indicates the beginning of the treatment.

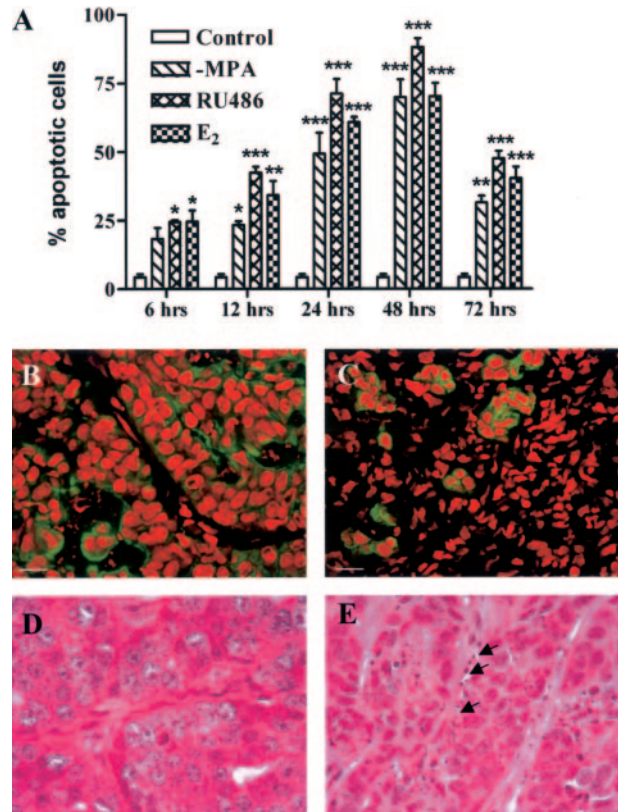


**Figure 3.** Loss of keratin-positive cells and increase in the percentage of apoptotic cells with the onset of regression. MPA depot was removed from BALB/c mice bearing the C4-HD tumor, and mice remained untreated (-MPA) or were additionally treated with  $E_2$  or RU486 for 6, 12, 24, 48, or 72 hours to induce tumor regression. Tumors were collected, fixed in 10% formalin, embedded in paraffin, and processed according to standard procedures to obtain H&E-stained sections. Apoptotic cells were counted under high magnification as explained in Materials and Methods. **A:** Number of apoptotic cells expressed as percentage over total number of cells per high-power field. There is a statistically significant increase in the percentage of apoptotic cells compared to the controls as early as 6 hours after the onset of treatments (\* $P \leq 0.05$ , \*\* $P \leq 0.01$ , \*\*\* $P \leq 0.001$ ). **B** and **C:** Immunofluorescence for pankeratin in frozen sections derived from control (**B**) and 72-hour RU486-treated (**C**) mice. Nuclei are stained with propidium iodide (red) and keratin with the corresponding primary antibody followed by a FITC-conjugated secondary antibody (green). Note the loss of keratin-positive cells in the samples derived from the treated mouse. Similar images were obtained from -MPA- and  $E_2$ -treated mice. **D** and **E:** High-magnification images obtained from H&E-stained sections derived from control (**D**) and 72-hour RU486-treated (**E**) mice. Note the presence of apoptotic cells next to the stromal compartment (**arrows**). The same result was observed by staining sections with the TUNEL reaction kit (not shown). Scale bars, 20  $\mu\text{m}$ . Original magnifications,  $\times 1000$  (**D**, **E**).

positive cells in tumor samples derived from untreated mice and, conversely, very few positive cells in samples obtained from 72-hour-treated mice (Figure 3, B and C, respectively). Close analysis of the H&E-stained sections at 6 and 12 hours of treatment showed that certain groups of dying cells were localized to the proximity of the stromal compartment (Figure 3E). Moreover, we were surprised to find a high degree of tissue remodeling that coincided with quick induction of apoptosis. Thus, based on the previous results, we wondered whether remodeling of ECM components and increases in MMP activity could be involved in the regression of the C4-HD tumor.

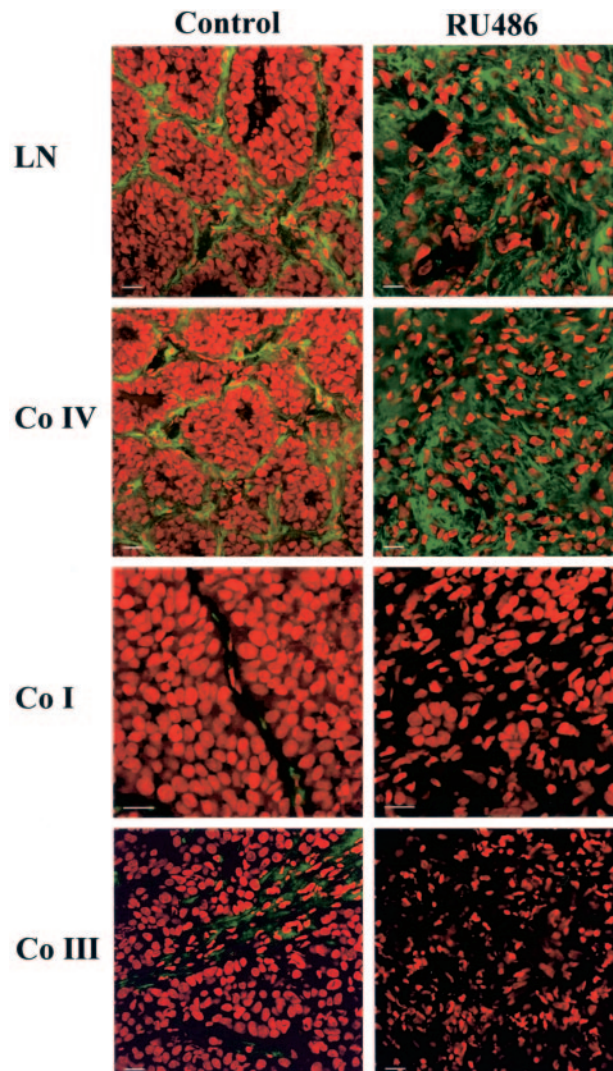


**Figure 4.** Remodeling of ECM components during tumor regression. Mice bearing the C4-HD tumor were treated for 72 hours by either removing MPA or adding E<sub>2</sub> or RU486 to induce regression. Samples were collected, frozen, and processed for immunofluorescence. Nuclei were stained with propidium iodide (red) and ECM components with the corresponding primary antibodies followed by FITC-conjugated secondary antibodies (green). The panels show staining for laminin (LN), collagen IV (Co IV), collagen I (Co I), and collagen III (Co III) in samples derived from control and 72-hour-treated RU486 mice. Note the change in ECM composition in the treated samples. The same pattern of staining was detected in tumors derived from animals treated by only removing MPA or by adding E<sub>2</sub> (not shown). Scale bars, 20  $\mu$ m.

#### ECM Remodeling and Proteolytic Activity Increase during Mammary Tumor Regression

In H&E-stained sections we found a high degree of tissue remodeling during regression. To confirm that ECM components were actually being modified, we analyzed the immunolocalization of the basement membrane components collagen IV and laminin together with the stromal collagens I and III by immunofluorescence. Figure 4 shows that in the growing C4-HD tumor laminin and collagen IV were very abundant with a thick basement membrane-like distribution that surrounded groups of epithelial

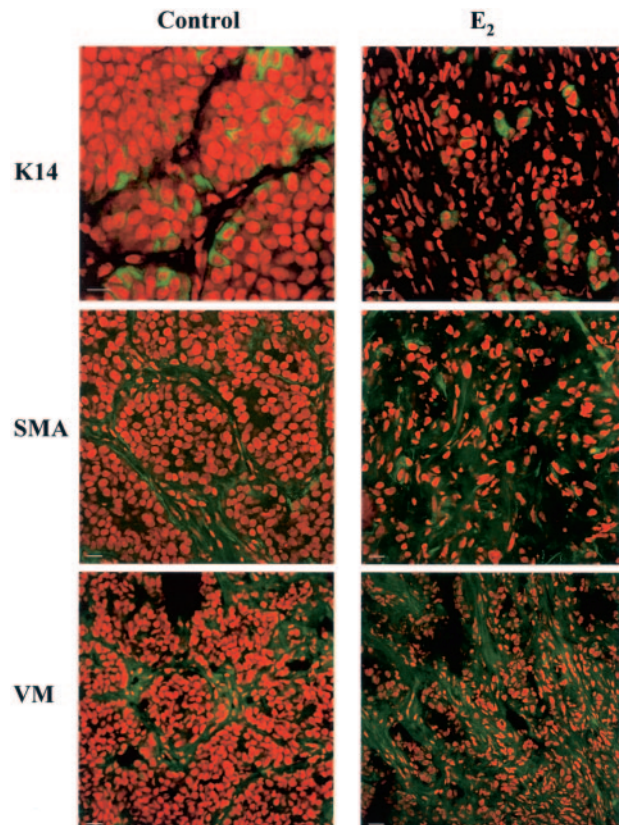


**Figure 5.** Characterization of cell types involved in the stromal reaction during regression. Tumors from control, -MPA-, E<sub>2</sub>-, and RU486-treated mice were collected at 72 hours. Samples were frozen and processed for immunofluorescence. Nuclei were stained with propidium iodide (red) and cytokeratin 14 (K14),  $\alpha$ -smooth muscle actin (SMA), and vimentin (VM) were detected using the corresponding primary antibodies followed by FITC-conjugated secondary antibodies (green). The samples shown correspond to 72-hour E<sub>2</sub>-treated samples. Similar results were obtained from samples derived from -MPA- and RU486-treated mice. An increase in VM- and SMA-positive cells was observed. K14-positive cells remained surrounded by fibroblast cells that were negative for this myoepithelial cell marker. Scale bars, 20  $\mu$ m.

elial cells (Figure 4). The stromal collagens I and III were less abundant but had a similar immunolocalization pattern to that of collagen IV and laminin (Figure 4). On the onset of regression, staining for both basement membrane components revealed that by 72 hours of treatment the original basement membrane-like structure was lost and that both laminin and collagen IV were still present in the tumor, intertwined between the stromal cells (Figure 4). However, at the same time point collagen I and III staining was practically undetectable (Figure 4). Our results thus revealed that basement membrane-like structures were present within the growing tumor and that both collagen IV and laminin were heavily remodeled during regression, accompanying the previously observed changes in tissue architecture. The analyzed stromal collagens, on the other hand, although present within the growing tumor, were lost on regression.

The loss of collagens I and III and the increase in the staining for basement membrane components strongly suggested that myoepithelial cells could be responsible for the fibrotic reaction observed during regression. To investigate if this was indeed the case, we performed

staining for K14, a myoepithelial cell marker. Unexpectedly, we found that a subpopulation of cells within the parenchyma of the growing tumor was positive for this cell marker (Figure 5). On regression we found a pattern of staining similar to that found for pankeratins, that is to say, groups of isolated cells within the increasing number of stromal-like cells. However, what drew our attention was the fact that the percentage of K14-positive cells within the regressing parenchyma was higher than that found in the growing tumor, where a low number of epithelial cells express this marker. In contrast vimentin and  $\alpha$ -smooth muscle actin staining showed that the stromal-like cells were positive for both these antigens and negative for K14 (Figure 5). Thus, these results together with those obtained for pankeratins suggested that fibroblasts, and not myoepithelial cells, were involved in the stromal reaction and in the production of laminin and collagen IV found in the regressing tumors. Interestingly, the detection of K14-positive cells within the tumor parenchyma and their enrichment during remission implied that these particular cells may be more resistant to treatment.

The remodeling of basement membrane components (laminin and collagen IV) and the loss of the stromal collagens strongly suggested that proteolytic activity could be up-regulated during the process of tumor regression. To investigate whether this was the case, MMP activity was analyzed by gelatin and casein zymography in tissue extracts of the C4-HD tumor during growth and regression. Gelatin zymography revealed bands corresponding to the previously described molecular weights of mouse mammary gland latent MMP-9 (LMMP-9) as well as active and latent MMP-2 (AMMP-2 and LMMP-2, respectively) (Figure 6A).<sup>22,23</sup> On the onset of regression, an increase in the levels of LMMP-9, LMMP-2, and AMMP-2 were detected in tumors derived from  $-$ MPA-, RU486-, and  $E_2$ -treated mice (Figure 6C). Compared to the controls, the differences were statistically significant as early as 24 hours for LMMP-9 in the  $-$ MPA-treated group and for LMMP-2 in the RU486-treated group. However, by 48 hours of treatment, all analyzed MMPs were increased significantly in samples derived from treated mice compared to their respective controls (Figure 6C). Surprisingly, this time point coincided with that of the highest levels of apoptosis as shown above. Casein zymography also revealed an increase in proteolytic activity with all treatments. Latent stromelysin-1 was detected and levels were up-regulated in samples derived from 72-hour-treated mice (Figure 6, B and C). Immunolocalization studies for LMMP-2 confirmed the zymography results, with staining for LMMP-2 low in control tumors and increased on regression (not shown). Thus, remodeling of basement membrane components and cell death during tumor regression occurred together with an increase in proteolytic activity. Moreover, we found that at 48 hours, when apoptosis reached its highest levels, gelatinases were significantly increased with all treatments.

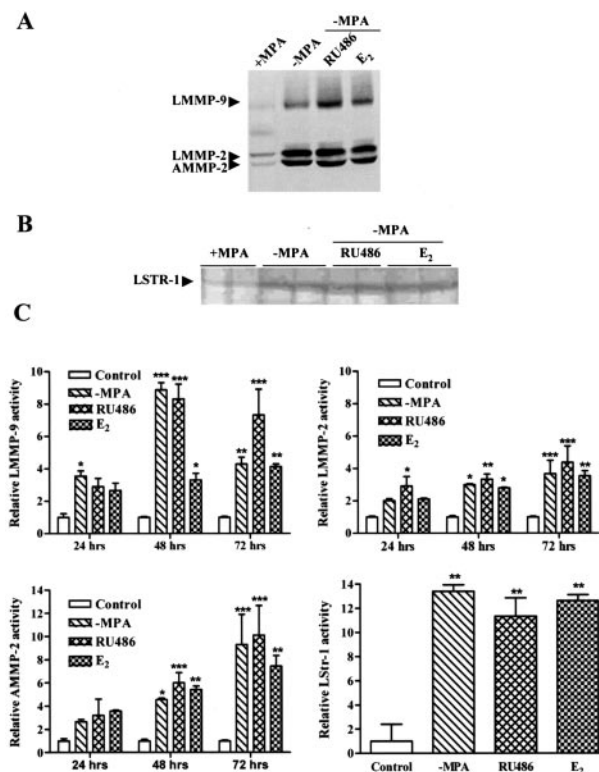


**Figure 6.** Increase in MMP activity during tumor regression. Tumors from control,  $-$ MPA-,  $E_2$ -, and RU486-treated mice were collected at 6, 12, 24, 48, and 72 hours. Tissues were processed for gelatin and casein zymography. **A:** A representative negative image of a gelatin zymogram for the 72-hour time point. Latent MMP-9 (LMMP-9) and latent and active forms of MMP-2 (LMMP-2, AMMP-2) were detected. **B:** A representative negative image of a casein zymogram for the 72-hour time point. Latent stromelysin-1 (LSTR-1) was detected. **C:** Densitometric analysis of samples derived from control and 24-, 48-, and 72-hour-treated mice for LMMP-9, LMMP-2, and AMMP-2. The panel showing the densitometric analysis of LSTR-1 corresponds to control and 72-hour-treated mice. In each case values represent the mean  $\pm$  SEM of samples derived from three mice. Values corresponding to 6- and 12-hour treatments are not shown because they were not statistically different from controls. Statistical significance of treated samples in relation to the corresponding control are shown as: \* $P \leq 0.05$ , \*\* $P \leq 0.01$ , \*\*\* $P \leq 0.001$ .

### Fragmentation and Loss of *E*-Cadherin during Tumor Regression

MMPs do not act only as regulators of ECM integrity but are also key players in modulating cell behavior. In particular MMP-2 and MMP-3 are capable of cleaving *E*-cadherin, thus affecting cell-cell interactions.<sup>24</sup> Because the C4-HD tumor expresses *E*-cadherin in the epithelial compartment, we investigated whether this molecule was lost or fragmented during regression. Figure 7 shows the staining pattern for *E*-cadherin in the growing C4-HD tumor and on 72 hours of regression. *E*-cadherin was specifically localized to the epithelial compartment in the growing tumor (Figure 7A); however, by 72 hours of regression very few *E*-cadherin-positive cells were detected (Figure 7B). This result was confirmed by Western blot using an antibody that recognizes the extracellular portion of *E*-cadherin. A 120-kd band was detected in tissue extracts derived from tumors grown in animals treated with MPA, but the band was lost after 72 hours of regression (Figure 8A). The same analysis was per-

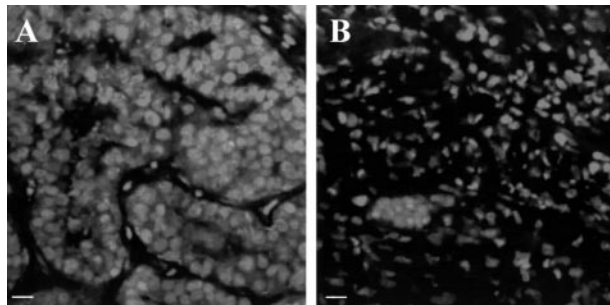


**Figure 7.** Loss of E-cadherin during tumor regression. Tumors from control, -MPA,  $E_2$ , and RU486-treated mice were collected at 72 hours. Samples were processed for immunofluorescence. Nuclei were stained with propidium iodide (red) and E-cadherin with the corresponding primary antibody followed by a FITC-conjugated secondary antibody. **A:** Staining for E-cadherin restricted to the epithelial compartment in the growing tumor. **B:** Very few E-cadherin-positive cells in a sample derived from an RU486-treated mouse. The same result was obtained in samples derived from -MPA- and  $E_2$ -treated mice (not shown). Scale bars, 20  $\mu\text{m}$ .

formed using an antibody directed against the intracellular portion of E-cadherin. Surprisingly, the samples derived from the control tumors revealed the presence of several bands together with the full-length 120-kd band (Figure 8B). This suggested that in the tumor there were multiple forms of E-cadherin. On regression, as observed

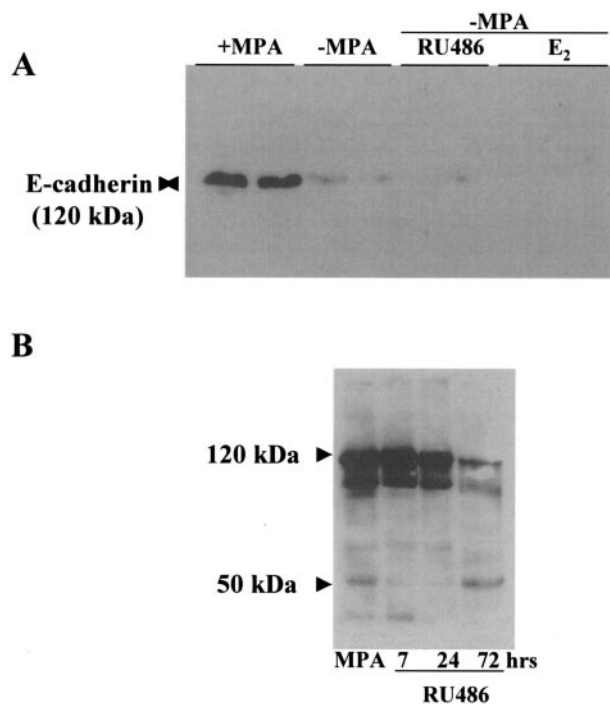


**Figure 8.** Fragmentation of E-cadherin during tumor regression. Tumors from control and -MPA-,  $E_2$ -, and RU486-treated mice were collected at 7, 24, and 72 hours. **A:** Western blot in which control samples were run together with samples derived from mice treated for 72 hours by either removing MPA (-MPA) or adding  $E_2$  or RU486. The Santa Cruz antibody was used in this case. A 120-kd band corresponding to the molecular weight of E-cadherin was detected in the control samples. On 72 hours of regression, the band was practically undetectable. **B:** Samples from control and 7-, 24-, and 72-hour RU486-treated mice run on an 8% gel. In this case the Transduction Laboratories antibody was used. Several isoforms of E-cadherin were detected using this antibody in control mice. On regression the high-molecular weight bands were reduced considerably and the 50-kd and other small molecular weight fragments were increased. Similar results were obtained with samples derived from -MPA- and  $E_2$  treated mice (not shown).

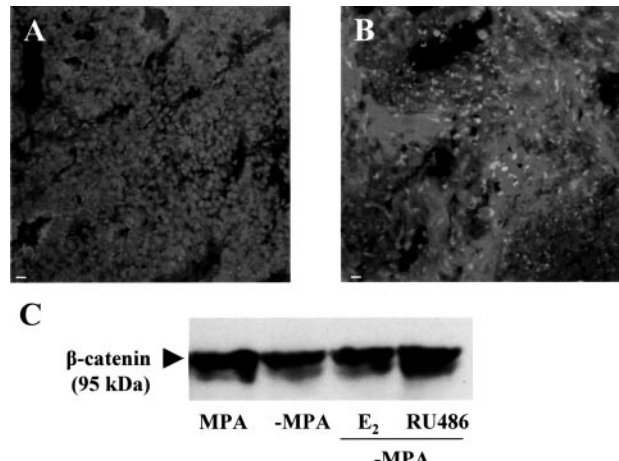


**Figure 9.**  $\beta$ -catenin levels are not reduced during tumor regression. Tumors from control and -MPA-,  $E_2$ -, and RU486-treated mice were collected at 72 hours. **A** and **B:** Immunofluorescence staining for  $\beta$ -catenin in samples derived from control and RU486-treated mice, respectively. **C:** Representative Western blot in which a control sample was run together with samples from -MPA-,  $E_2$ -, and RU486-treated samples. No differences were detected between the control and treated samples. A doublet at 95 kd was detected as described by other authors.<sup>33</sup> Scale bars, 20  $\mu\text{m}$ .

with the first antibody, there was a decrease in the intensity of the 120-kd band. Moreover, we detected an increase in the lower molecular weight fragments of E-cadherin, especially the 50-kd isoform (Figure 8C). Thus, the fragmentation of E-cadherin observed during regression, which coincided temporally with the increase in MMP activity and apoptosis, strongly suggested that the increase in proteolysis was not an epiphenomenon but that it played a role during tumor regression.

### $\beta$ -Catenin Is Involved in the Stromal Reaction that Accompanies Tumor Regression

Given the loss observed in E-cadherin during tumor regression, we next investigated the immunolocalization of  $\beta$ -catenin. As expected, in the growing tumor  $\beta$ -catenin was localized to the cell membrane in the epithelial compartment (Figure 9A). Treatment by removing MPA or additionally treating with either RU486 or  $E_2$  to induce regression resulted in a change in the immunolocalization of  $\beta$ -catenin, with staining reduced at the cell membranes (in coincidence with the loss of epithelial cells) and increased in the cytoplasm of the stromal cells that arose as regression progressed (Figure 9B). Western blot analysis confirmed these observations because total levels of  $\beta$ -catenin did not decrease as regression progressed (Figure 9C). These results reveal distinct roles for  $\beta$ -catenin during tumor growth and regression at the level of epithelial adhesion in the former and in the process of stromal reaction in the latter.

### Discussion

The goal of the present study was to define the events involved in the early hours of mammary tumor regression related to changes in the ECM, proteolytic activity, and

cell-cell interactions. Our study is the first, to our knowledge, to show that during tumor regression the increase in cell death is accompanied by an increase in proteolytic activity and ECM remodeling. Moreover, the fragmentation and loss of E-cadherin strongly suggest that the increase in proteolytic activity could be responsible not only for altering cell-matrix interactions but also cell-cell adhesion. Both events could thus lead to apoptosis and loss of tumor mass. Proteolytic activity has traditionally been linked to tumor progression and invasion in cancer biology. However, the concept that tumor shrinkage is associated with an increase in proteolytic activity is not surprising considering that proteolysis has already been shown to play a role in mammary gland involution, a process in which apoptosis is followed by a loss of tissue mass. Our work does not contradict previous findings but rather questions the rationale for the development of MMP inhibitors with the aim of reducing tumor burden.

We had previously shown that hormone-induced regression is characterized by an increase in apoptosis.<sup>19</sup> Likewise, analysis of the C4-HD tumors revealed that as early as 6 hours there was a statistically significant increase in the percentage of apoptotic cells. The highest levels of apoptosis were detected at 48 hours for all treatments, with values ranging ~90% for the RU486-treated group and 70% for the -MPA- and E<sub>2</sub>-treated groups. This phenomenon was characterized by evident changes in the stromal compartment in the form of fibrosis, which has previously been shown in experimental and human tumors to accompany reductions in tumor size.<sup>19,25</sup>

The results concerning the changes in the stromal compartment prompted us to analyze the composition of the ECM in samples derived from untreated and treated mice. We found that laminin and collagen IV had a thick basement membrane-like distribution in the growing tumors, localized to the stromal-cancer epithelial interface, as previously shown by others for laminin-1 in human breast tumors.<sup>26</sup> On 72 hours of treatment, this organization was completely lost, and a disorganized lattice of laminin and collagen IV now covered the tissue sections. On the other hand, the stromal collagens I and III were less abundant in the growing tumor, and the staining for both was lost on regression. This result was puzzling given that we expected to find similarities with the process of wound healing, during which fibrosis is characterized by deposition of the stromal collagens I and III.<sup>27</sup> The finding that collagen IV and laminin were very abundant in the samples derived from treated mice raised the issue of the lineage of the tumor and stromal cells. Basement membrane components such as collagen IV and laminin are indicative of the presence of myoepithelial cells in the mouse mammary gland.<sup>28</sup> We thus performed stainings to pankeratins, K14,  $\alpha$ -smooth muscle actin, and vimentin. In the epithelial compartment of the growing tumor, there was a subpopulation of K14-positive cells that were  $\alpha$ -smooth muscle actin-negative, thus ruling out a myoepithelial identity. The fibroblastic cells were positive for vimentin and  $\alpha$ -smooth muscle actin in both growing and regressing tissues. We do not know the origin of these fibroblastic cells or whether they were truly

responsible for the synthesis and deposition of the basement membrane components. Future studies aimed at establishing their molecular identity may answer if they have originated within the tumor or in the bone marrow. The discovery that most epithelial cells present in the 72-hour-treated samples were K14-positive suggests that this particular cell population may be more resistant to apoptosis.

The finding that there is a change in the organization of the basement membrane during regression strongly supported the involvement of proteolytic activity in the process of tumor regression. Deposition of ECM components does not require proteolytic activity, but the change in their arrangement does because three-dimensional structures must be replaced. Accordingly, during regression there was an increase in the levels of LMMP-9, LMMP-2, and AMMP-2 and latent stromelysin-1. Our findings show that in our model system tumor regression is reminiscent of mammary gland lactational involution. MMPs have been shown to be up-regulated during post-lactational involution and to play a key role in the process of apoptosis that enables the shrinkage of the tissue and the re-establishment of the nonlactating mammary structure.<sup>13,14</sup> The finding that certain groups of apoptotic cells localized adjacent to the basement membrane-like structures in the tumor as regression progressed strongly suggested an important role for anoikis in the response of the tumor to the hormone treatment. We believe that in this tumor model in particular, the primary target of the treatments is the epithelium, given that the malignant cells express ER and PR.<sup>17</sup> However, a secondary stromal reaction as a consequence of epithelial-stromal interactions may determine the effectiveness of the hormone therapy.

The peak in apoptosis for all three treatments coincided with the time point at which MMP activity raised significantly from controls. The fact that apoptosis levels began to increase significantly from controls before the rise in proteolytic activity may suggest two phases of apoptosis: one early and independent of proteolytic activity and a second phase that is dependent on proteolysis, as has been shown for mammary gland involution.<sup>14</sup> In view of our results, and given the fact that to date clinical trials using synthetic MMP inhibitors have failed,<sup>8</sup> we believe that proteolytic activity may have a key role in tumor shrinkage just as in tumor development. We are currently performing experiments to test whether the inhibition of MMP activity hampers tumor regression in our model system. If our hypothesis is correct, it would give a rational explanation to the lack of positive results in the clinic.

MMPs have been previously shown to affect cell-cell interactions by degrading E-cadherin;<sup>24</sup> we thus investigated whether this molecule was degraded during regression. As identified by an antibody recognizing the extracellular domain, E-cadherin was practically lost by 72 hours of treatment in our model. This correlated with a steady increase of lower molecular weight isoforms of the protein, a phenomenon that could be the result of cleavage by proteolytic activity or alterations in the synthesis and/or processing of the molecule, as has been previ-

ously described for prostate cancer epithelial cells.<sup>29,30</sup> Rios-Doria and colleagues<sup>31</sup> reported cleavage of the 35-kd intracellular  $\beta$ -catenin binding site of E-cadherin in the early hours of involution, which was actually performed by calpain. Using the same antibody we used in our studies, they showed that the 35-kd fragment increased as involution progressed. We believe that tumor regression and mammary gland involution, although mechanistically different, lead to a loss of function of E-cadherin that could be responsible not only for affecting tissue structure but also for induction of apoptosis, as shown in other model systems.<sup>32</sup>

Having found that E-cadherin levels were radically diminished during regression, we expected to find a loss of  $\beta$ -catenin as well. This, however, was not the case. A closer analysis revealed that although the epithelial compartment of the tumor was lost during regression and  $\beta$ -catenin was no longer localized at sites of epithelial cell-cell junctions, there was a dramatic increase in the expression of this molecule in the stromal cells. Thus, our results suggest that  $\beta$ -catenin could have a role in the stromal reaction that accompanies loss of the epithelial compartment of the tumor. This is further supported by the fact that  $\beta$ -catenin has been found by others to play a key role in the proliferative phase of wound healing.<sup>33</sup> Cheon and collaborators<sup>33</sup> further showed that the over-expression of  $\beta$ -catenin in mesenchymal cells leads to aggressive fibromatoses and hyperplastic cutaneous wounds. The cytoplasmatic accumulation of  $\beta$ -catenin in the stromal cells during regression could reflect a positive regulation of Wnt expression in the tissue, as has been shown for Wnt 4 in early wound healing.<sup>34</sup> Alternatively, other factors involved in the early hours of regression could be involved in the stabilization of  $\beta$ -catenin. Either way, we hypothesize that, like during wound healing, the early phases of tumor regression may be characterized by an increase in Tcf-dependent transcription that likely regulates the expression of genes important in the remodeling phase described in this article. It is interesting to point out that, although the results concerning ECM composition during regression seemed to imply a mechanism different to the one described for wound healing, our findings regarding  $\beta$ -catenin suggest that there could be similarities in the signaling pathways responsible for the stromal reaction.

Finally, all three treatments yielded similar results concerning proteolytic activity, ECM composition, and cell-cell interactions. The groups treated by only removing MPA usually took more time to regress completely. This coincided with the fact that the induction of apoptosis in this group was statistically different from the controls at 12 hours and the RU486 and E<sub>2</sub> groups, which showed differences as early as 6 hours. We have not yet analyzed the signaling pathways in this particular tumor in response to these three treatments, but we suspect that RU486 and E<sub>2</sub> additionally block the PR signaling pathway. This pathway may not be completely shut down by only removing MPA, because the mice we work with are not ovariectomized and thus endogenous levels of progesterone persist.

Our results show a novel role for proteolytic activity in tumor regression in an *in vivo* model of mouse mammary cancer. We believe that the changes observed in the ECM and in the stromal cells themselves are as important to tumor shrinkage as the death of the neoplastic cells. Moreover, they suggest that stromal-epithelial interactions are key to the outcome of tumor therapy, raising doubts as to the use of MMP inhibitors for the treatment of cancer.

### Acknowledgments

We thank Julieta Bolado for technical support and Gador Laboratories for providing MPA.

### References

1. Parkin DM: International variation. *Oncogene* 2004, 23:6329–6340
2. Lacey Jr JV, Devesa SS, Brinton LA: Recent trends in breast cancer incidence and mortality. *Environ Mol Mutagen* 2002, 39:82–88
3. Werb Z: ECM and cell surface proteolysis: regulating cellular ecology. *Cell* 1997, 91:439–442
4. Sternlicht MD, Werb Z: How matrix metalloproteinases regulate cell behavior. *Annu Rev Cell Dev Biol* 2001, 17:463–516
5. Egeblad M, Werb Z: New functions for the matrix metalloproteinases in cancer progression. *Nat Rev Cancer* 2002, 2:161–174
6. Liotta LA, Kohn EC: The microenvironment of the tumour-host interface. *Nature* 2001, 411:375–379
7. Coussens LM, Tinkle CL, Hanahan D, Werb Z: MMP-9 supplied by bone marrow-derived cells contributes to skin carcinogenesis. *Cell* 2000, 103:481–490
8. Coussens LM, Fingleton B, Matrisian LM: Matrix metalloproteinase inhibitors and cancer: trials and tribulations. *Science* 2002, 295:2387–2392
9. Lanari C, Molinolo AA, Pasqualini CD: Induction of mammary adenocarcinomas by medroxyprogesterone acetate in BALB/c female mice. *Cancer Lett* 1986, 33:215–223
10. Molinolo AA, Lanari C, Charreau EH, Sanjuan N, Pasqualini CD: Mouse mammary tumors induced by medroxyprogesterone acetate: immunohistochemistry and hormonal receptors. *J Natl Cancer Inst* 1987, 79:1341–1350
11. Kordon E, Lanari C, Molinolo AA, Elizalde PV, Charreau EH, Dosne PC: Estrogen inhibition of MPA-induced mouse mammary tumor transplants. *Int J Cancer* 1991, 49:900–905
12. Montecchia MF, Molinolo A, Lanari C: Reversal of estrogen-resistance in murine mammary adenocarcinomas. *Breast Cancer Res Treat* 1999, 54:93–99
13. Talhouk RS, Bissell MJ, Werb Z: Coordinated expression of extracellular matrix-degrading proteinases and their inhibitors regulates mammary epithelial function during involution. *J Cell Biol* 1992, 118:1271–1282
14. Lund LR, Romer J, Thomasset N, Solberg H, Pyke C, Bissell MJ, Dano K, Werb Z: Two distinct phases of apoptosis in mammary gland involution: proteinase-independent and -dependent pathways. *Development* 1996, 122:181–193
15. Boudreau N, Sympson CJ, Werb Z, Bissell MJ: Suppression of ICE and apoptosis in mammary epithelial cells by extracellular matrix. *Science* 1995, 267:891–893
16. Institute of Laboratory Animal Resources CoLSNRC: Guide for the Care and Use of Laboratory Animals. Washington, DC, National Academy Press, 1996
17. Lanari C, Luthy I, Lamb CA, Fabris V, Pagano E, Helguero LA, Sanjuan N, Merani S, Molinolo AA: Five novel hormone-responsive cell lines derived from murine mammary ductal carcinomas: *in vivo* and *in vitro* effects of estrogens and progestins. *Cancer Res* 2001, 61:293–302
18. Lanari C, Montecchia MF, Pazos P, Simian M, Vanzulli S, Lamb C, Molinolo AA: Progestin-induced mammary adenocarcinomas in

- BALB/c mice. Progression from hormone-dependent to autonomous tumors. *Medicina (B Aires)* 1997, 57(Suppl 2):55–69
19. Vanzulli S, Efeyan A, Benavides F, Helguero LA, Peters G, Shen J, Conti CJ, Lanari C, Molinolo A: p21, p27 and p53 in estrogen and antiprogestin-induced tumor regression of experimental mouse mammary ductal carcinomas. *Carcinogenesis* 2002, 23:749–758
  20. Horwitz KB, Tung L, Takimoto GS: Novel mechanisms of antiprogestin action. *Acta Oncol* 1996, 35:129–140
  21. Kerr JF, Wyllie AH, Currie AR: Apoptosis: a basic biological phenomenon with wide-ranging implications in tissue kinetics. *Br J Cancer* 1972, 26:239–257
  22. Talhouk RS, Chin JR, Unemori EN, Werb Z, Bissell MJ: Proteinases of the mammary gland: developmental regulation in vivo and vectorial secretion in culture. *Development* 1991, 112:439–449
  23. Simian M, Hirai Y, Navre M, Werb Z, Lochter A, Bissell MJ: The interplay of matrix metalloproteinases, morphogens and growth factors is necessary for branching of mammary epithelial cells. *Development* 2001, 128:3117–3131
  24. Lochter A, Galosy S, Muschler J, Freedman N, Werb Z, Bissell MJ: Matrix metalloproteinase stromelysin-1 triggers a cascade of molecular alterations that leads to stable epithelial-to-mesenchymal conversion and a premalignant phenotype in mammary epithelial cells. *J Cell Biol* 1997, 139:1861–1872
  25. Miller WR, Dixon JM, Macfarlane L, Cameron D, Anderson TJ: Pathological features of breast cancer response following neoadjuvant treatment with either letrozole or tamoxifen. *Eur J Cancer* 2003, 39:462–468
  26. Gudjonsson T, Ronnov-Jessen L, Villadsen R, Rank F, Bissell MJ, Petersen OW: Normal and tumor-derived myoepithelial cells differ in their ability to interact with luminal breast epithelial cells for polarity and basement membrane deposition. *J Cell Sci* 2002, 115:39–50
  27. Scheithauer M, Riechelmann H: Basic mechanisms of cutaneous woundhealing. *Laryngorhinootologie* 2003, 82:31–35
  28. Petersen OW, Nielsen HL, Gudjonsson T, Villadsen R, Rank F, Niebuhr E, Bissell MJ, Ronnov-Jessen L: Epithelial to mesenchymal transition in human breast cancer can provide a nonmalignant stroma. *Am J Pathol* 2003, 162:391–402
  29. Rashid MG, Sanda MG, Vallorosi CJ, Rios-Doria J, Rubin MA, Day ML: Posttranslational truncation and inactivation of human E-cadherin distinguishes prostate cancer from matched normal prostate. *Cancer Res* 2001, 61:489–492
  30. Kuefer R, Hofer MD, Gschwend JE, Pienta KJ, Sanda MG, Chinnaiyan AM, Rubin MA, Day ML: The role of an 80 kDa fragment of E-cadherin in the metastatic progression of prostate cancer. *Clin Cancer Res* 2003, 9:6447–6452
  31. Rios-Doria J, Day KC, Kuefer R, Rashid MG, Chinnaiyan AM, Rubin MA, Day ML: The role of calpain in the proteolytic cleavage of E-cadherin in prostate and mammary epithelial cells. *J Biol Chem* 2003, 278:1372–1379
  32. Day ML, Zhao X, Vallorosi CJ, Putzi M, Powell CT, Lin C, Day KC: E-cadherin mediates aggregation-dependent survival of prostate and mammary epithelial cells through the retinoblastoma cell cycle control pathway. *J Biol Chem* 1999, 274:9656–9664
  33. Cheon SS, Nadesan P, Poon R, Alman BA: Growth factors regulate beta-catenin-mediated TCF-dependent transcriptional activation in fibroblasts during the proliferative phase of wound healing. *Exp Cell Res* 2004, 293:267–274
  34. Labus MB, Stirk CM, Thompson WD, Melvin WT: Expression of Wnt genes in early wound healing. *Wound Repair Regen* 1998, 6:58–64